

Supporting Information

Chromism of Bi₂WO₆ in Single Crystal and Nanosheet Forms

Timothy R. Pope, Melissa N. Lassig, Gregory Neher, Richard D. Weimar III,
and Tina T. Salguero*

*Department of Chemistry
The University of Georgia
salguero@uga.edu*

Synthesis of $\text{Cs}_4\text{W}_{11}\text{O}_{36}^{2-}$ Nanosheets

Materials: Cs_2CO_3 (99% trace metal basis), WO_3 (99% trace metal basis), and $\text{Bi}(\text{NO}_3)_3 \cdot 5\text{H}_2\text{O}$ (98% reagent grade) were purchased from the Sigma-Aldrich Corp. All reagents were used as received.

This procedure is based on that reported by Sasaki and co-workers.^{S1} Cs_2CO_3 and WO_3 were ground together in a molar ratio of 4:11 using an agate mortar and pestle for 5 min. The resulting yellow powder was placed in a platinum crucible and heated at 900 °C for 5 hours. Reflective silver crystals of $\text{Cs}_{6+x}\text{W}_{11}\text{O}_{36}$ were removed from the platinum crucible using 12 M HCl and mild bath sonication for 30 min to 1 hr. Typical yields are ~85%. After grinding these crystals into a dull grey powder, 7 g of this material were added to 600 mL of 12 M HCl and agitated on an orbital shaker at 180 rpm for 2 days at room temperature. The resulting mixture was allowed to settle; the grey solids are $\text{Cs}_{6+x}\text{W}_{11}\text{O}_{36}$ and the white dispersion consists of $\text{Cs}_4\text{W}_{11}\text{O}_{36}^{2-}$ nanosheets. The white supernatant was decanted from the solids, and the nanosheets were isolated by centrifugation at 10,000 rpm for 20 min (4x, replacing the acid with fresh water each time, taking care to keep the sample very concentrated, and dispersing by bath sonication). The final pearlescent white dispersion is shown in Fig. S1. Additional exfoliated material could be collected by repeating the acid treatment-agitation-centrifugation cycles 4x. Typical isolated yields of $\text{Cs}_4\text{W}_{11}\text{O}_{36}^{2-}$ nanosheets are ~15%.



Figure S1. Pearlescent distortions of a stirred, aqueous dispersion of $\text{Cs}_4\text{W}_{11}\text{O}_{36}^{2-}$ nanosheets.

Additional Characterization of $\text{Cs}_4\text{W}_{11}\text{O}_{36}^{2-}$ Nanosheets

AFM samples were prepared by diluting an aqueous $\text{Cs}_4\text{W}_{11}\text{O}_{36}^{2-}$ nanosheet dispersion with isopropanol and drop casting onto a silicon wafer. Topographic images were obtained using a Bruker Innova microscope.

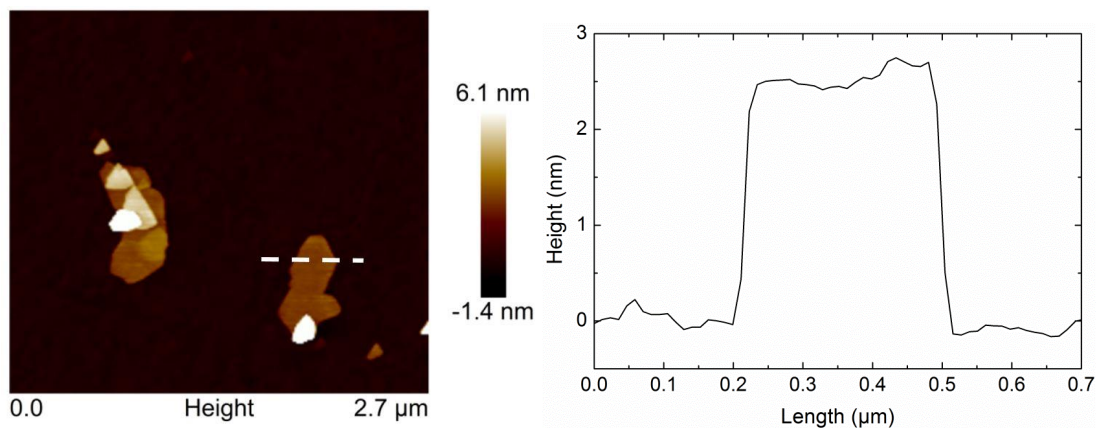


Figure S2. AFM characterization of $\text{Cs}_4\text{W}_{11}\text{O}_{36}^{2-}$ nanosheets.

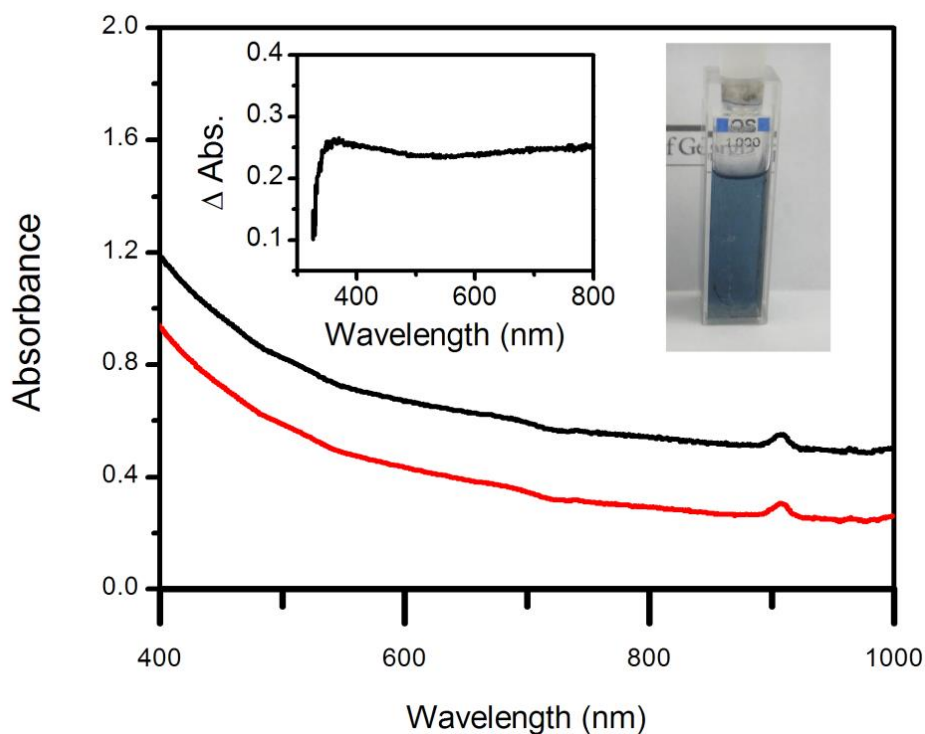


Figure S3. UV-Vis data for exfoliated $\text{Cs}_4\text{W}_{11}\text{O}_{36}^{2-}$ nanosheets (6.7×10^{-5} M aqueous solution) before (black curve) and after (red curve) UV irradiation. Inset plot shows the absorbance gain. Photo inset shows the blue color of a $\text{Cs}_4\text{W}_{11}\text{O}_{36}^{2-}$ nanosheet dispersion after UV irradiation.

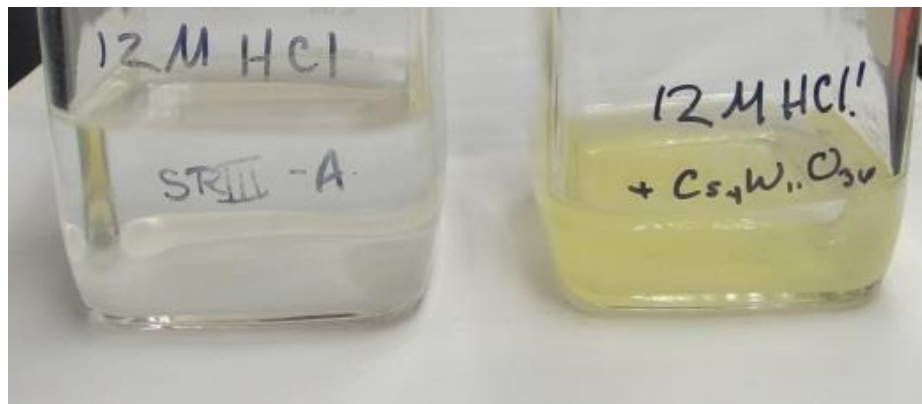


Figure S4. Left: exfoliated $\text{Cs}_4\text{W}_{11}\text{O}_{36}^{2-}$ nanosheets. Right: yellow (re-stacked) $\text{Cs}_4\text{W}_{11}\text{O}_{36}^{2-}$ nanosheets.

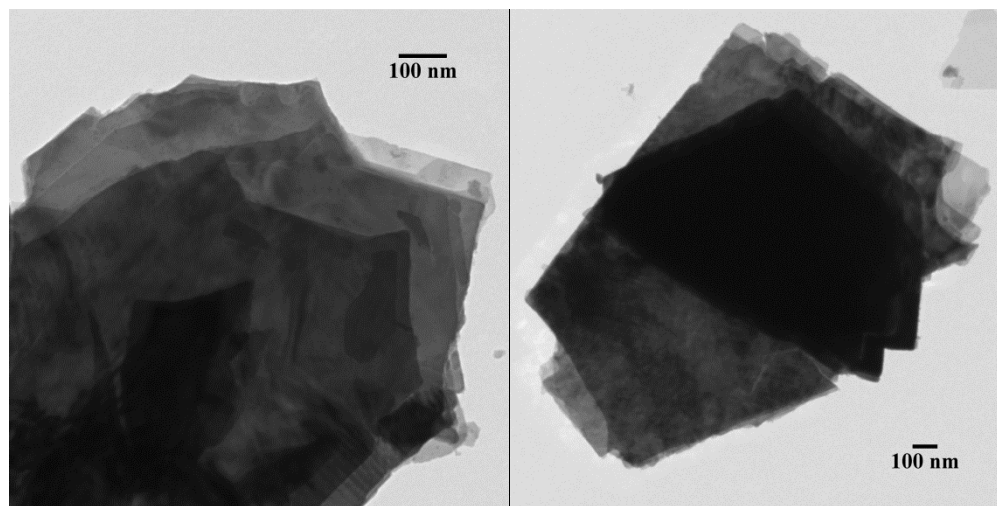


Figure S5. Representative TEM images of material from the yellow (re-stacked) $\text{Cs}_4\text{W}_{11}\text{O}_{36}^{2-}$ nanosheet samples.

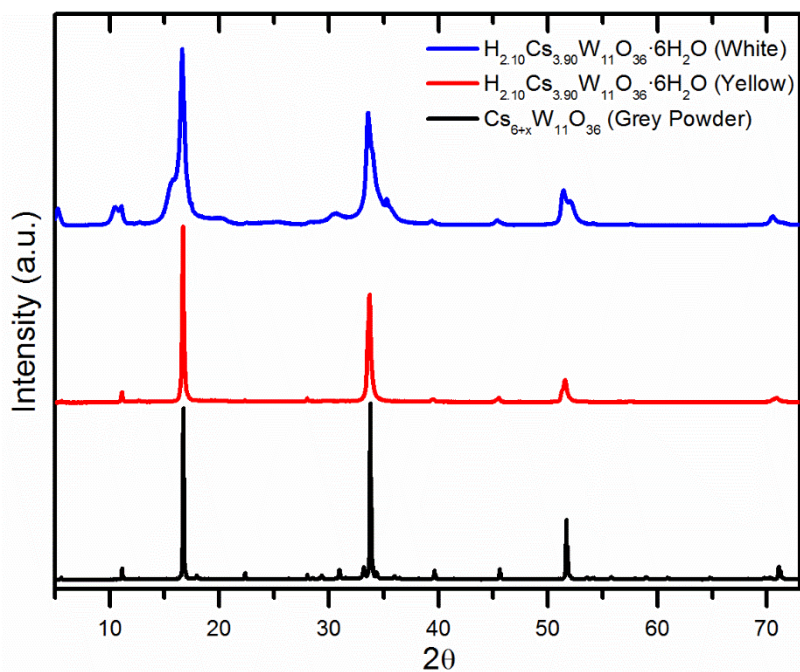


Figure S6. Comparison of PXRD data for $\text{Cs}_{6+x}\text{W}_{11}\text{O}_{36}$ (black pattern), white exfoliated $\text{Cs}_4\text{W}_{11}\text{O}_{36}^{2-}$ nanosheets (blue pattern), and yellow (re-stacked) $\text{Cs}_4\text{W}_{11}\text{O}_{36}^{2-}$ nanosheets (red pattern).

Additional Characterization of Bi₂WO₆ Nanosheets

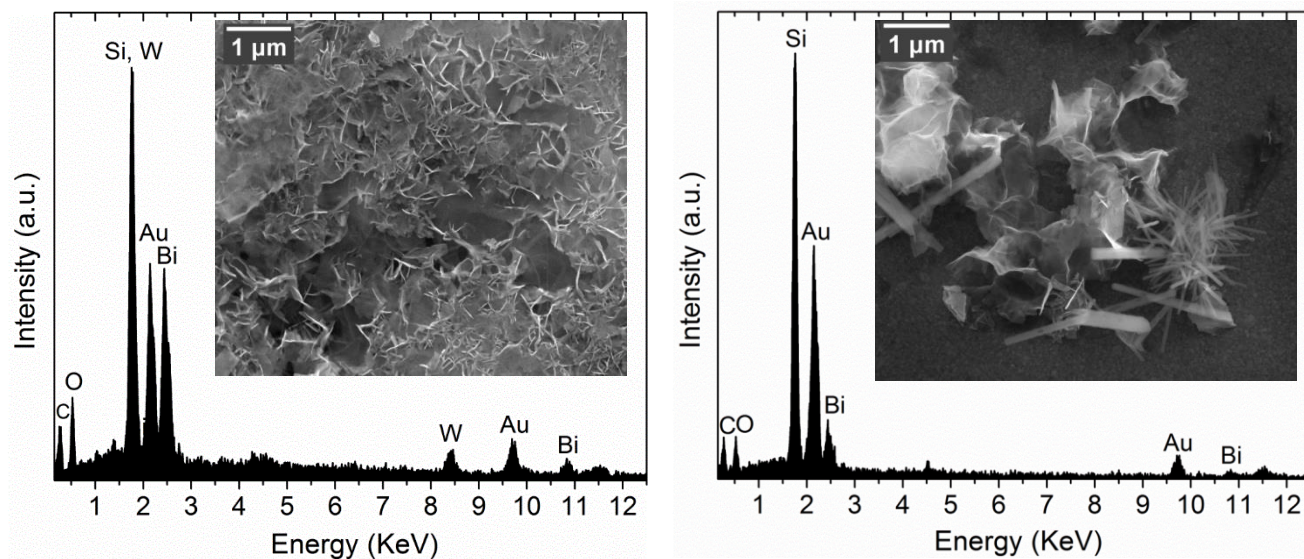


Figure S7. SEM images and EDS analysis of the reaction mixture at the 2 hr mark.
Note the rods of bismuth oxide visible in the sample at right.

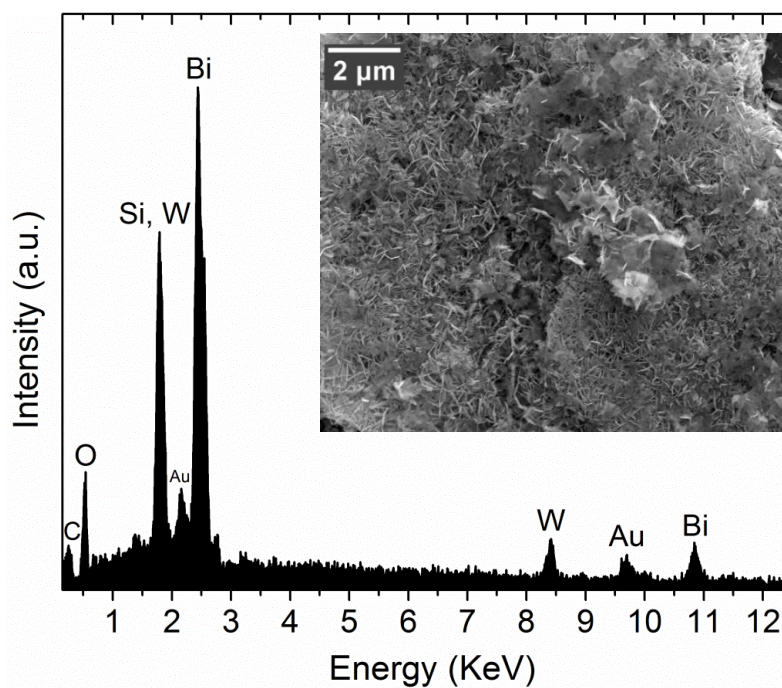


Figure S8. SEM images and EDS analysis of the reaction mixture at the 6 hr mark.



Figure S9. Left: powder sample of Bi_2WO_6 nanosheets. Right: an aqueous dispersion of Bi_2WO_6 nanosheets that exhibits pearlescent distortions when agitated (by stirring in this case).

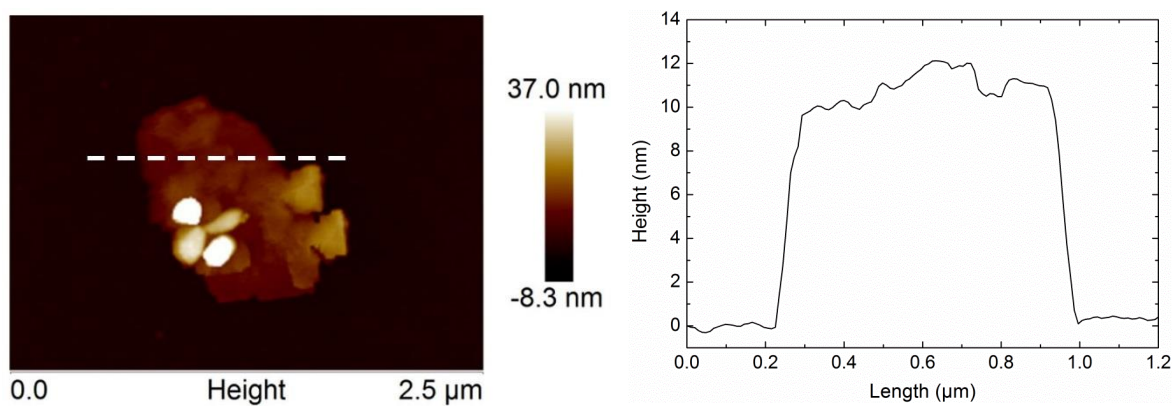


Figure S10. AFM characterization of Bi_2WO_6 nanosheets.

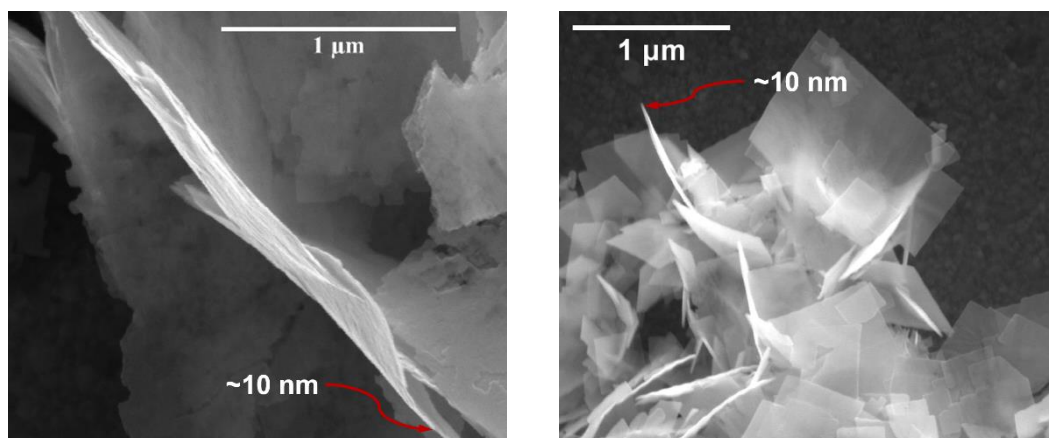


Figure S11. SEM images of Bi₂WO₆ nanosheets used to estimate their average thickness.

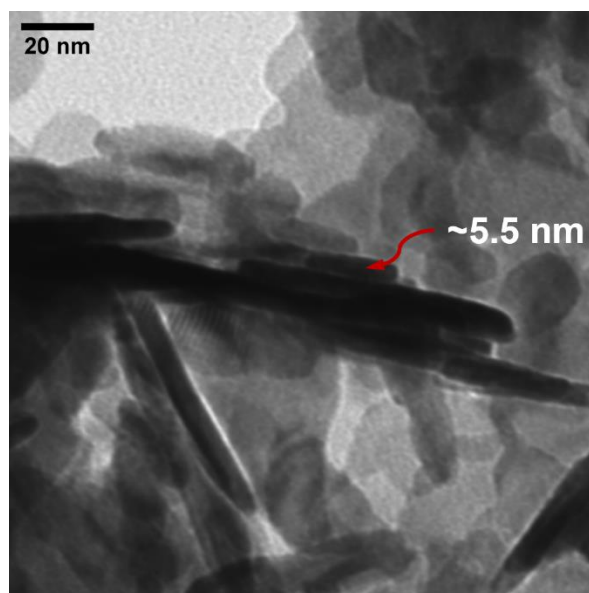


Figure S12. TEM image of Bi₂WO₆ nanosheets used to estimate their average thickness.

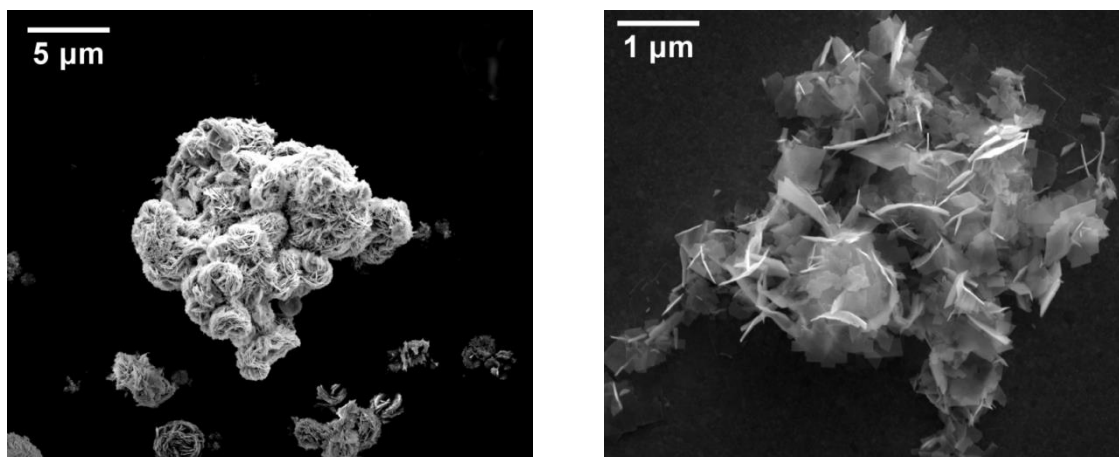


Figure S13. Left: SEM image of flowerlike Bi_2WO_6 nanosheet clusters prepared by a literature procedure.^{S2} Right: SEM image of a loose aggregate of Bi_2WO_6 nanosheets, those reported in this work.

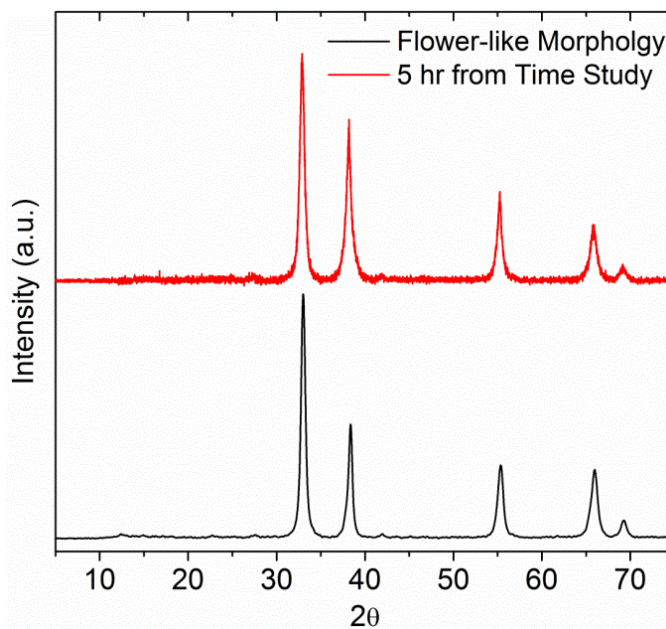


Figure S14. PXRD data from a sample of flowerlike Bi_2WO_6 nanosheet clusters prepared by a literature procedure,^{S2} compared with Bi_2WO_6 nanosheets reported in this work (isolated after 5 hrs reaction, part of the time study).

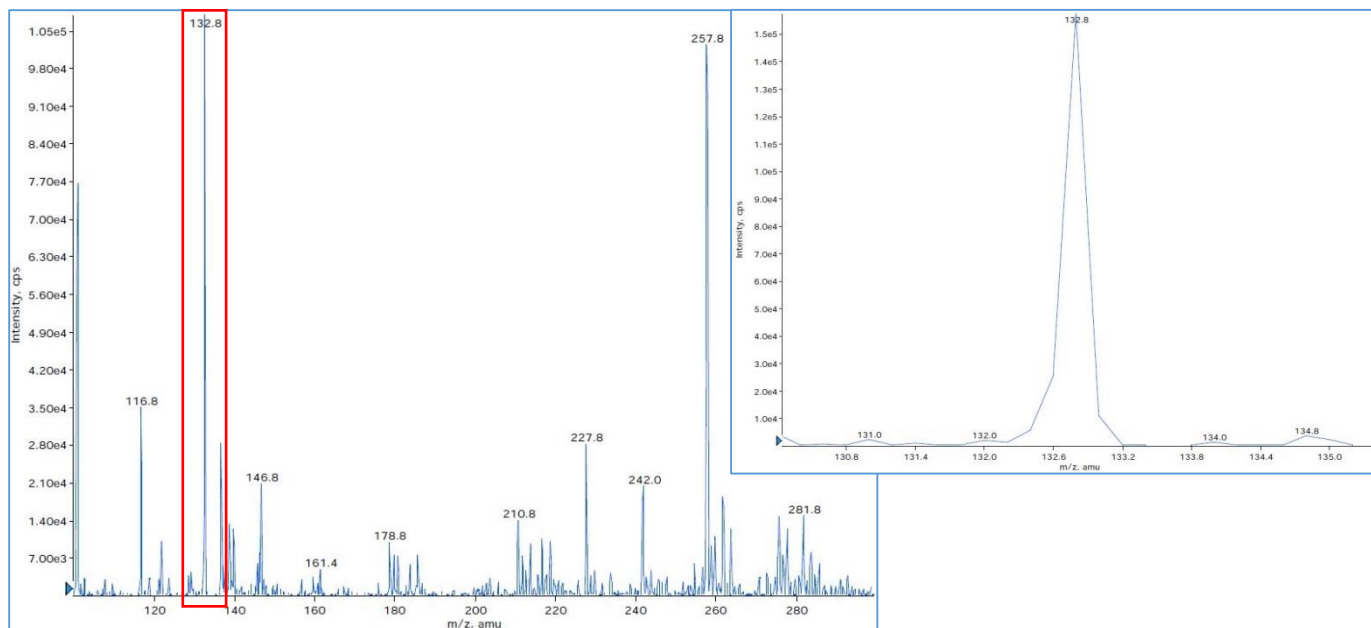


Figure S15. ESI-MS data that identifies Cs^+ in the filtrate collected while isolating the Bi_2WO_6 nanosheet product.

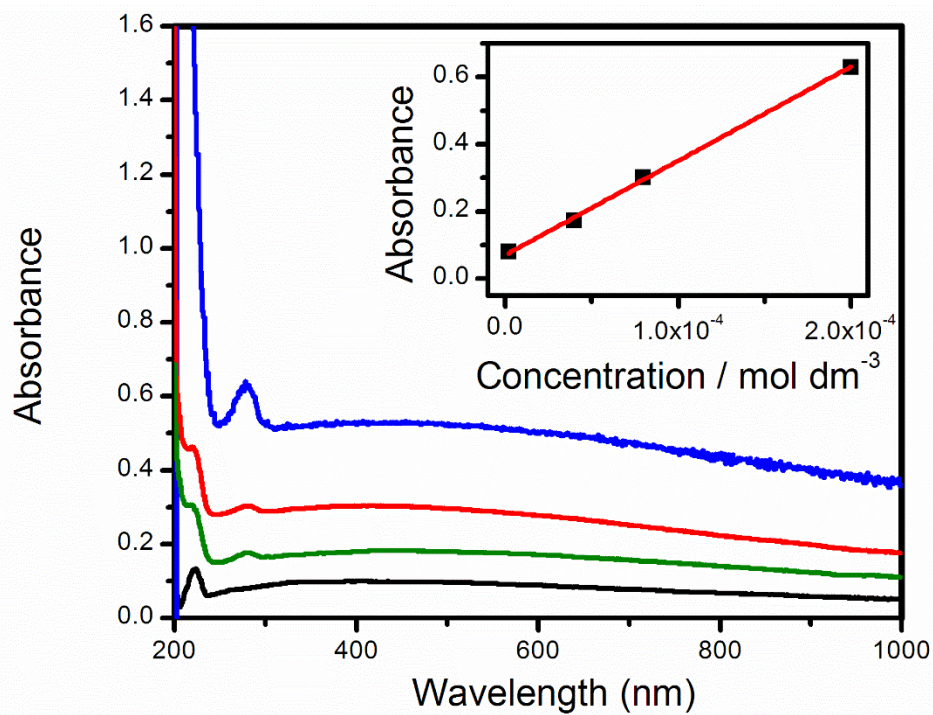


Figure S16. Absorbance data of Bi_2WO_6 nanosheets at varying concentrations; inset shows the absorbance vs. concentration curve used to determine the molar extinction coefficient at 281 nm.

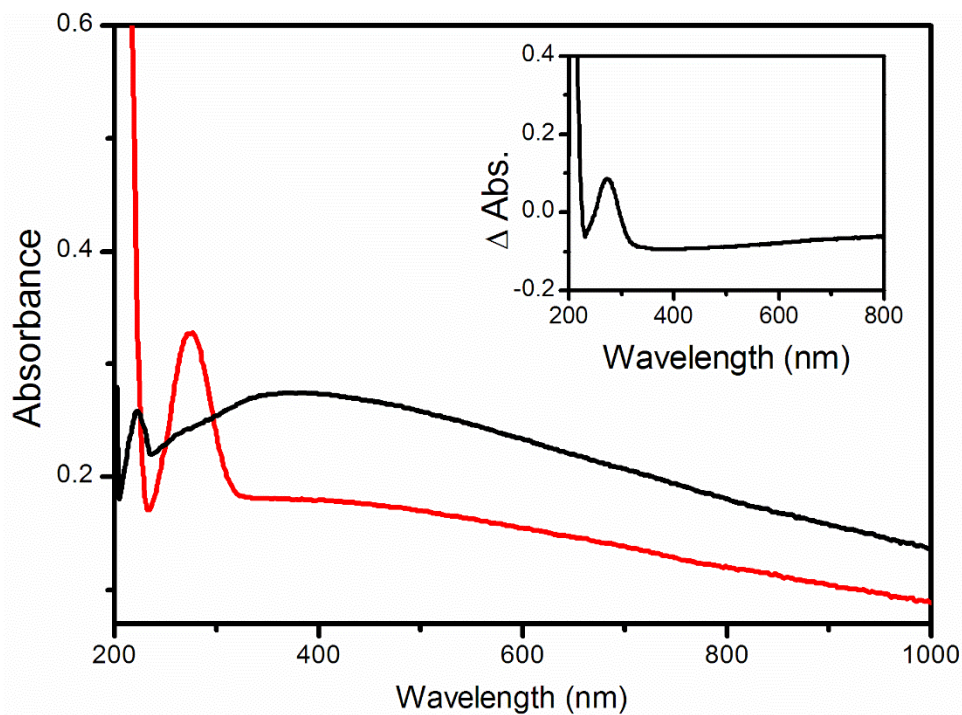


Figure S17. Absorption spectra of an aqueous dispersion of Bi_2WO_6 nanosheets ($6.7 \times 10^{-5} \text{ M}$) before (black curve) and after UV irradiation (red curve). Inset plot: change in absorbance before and after UV-irradiation

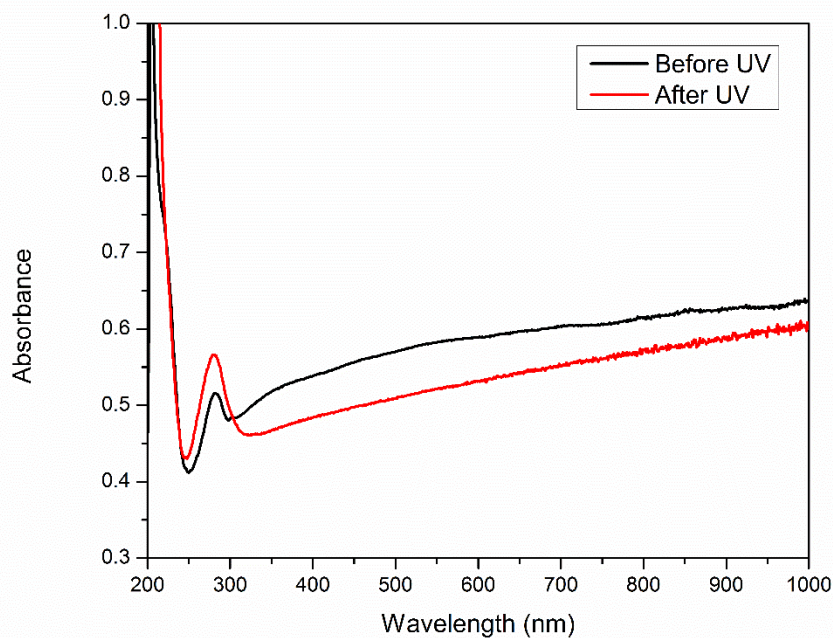
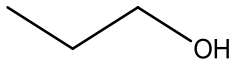
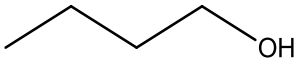
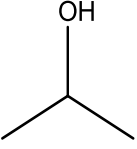
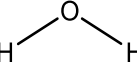
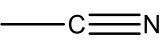
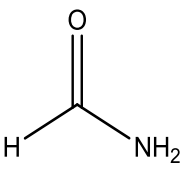
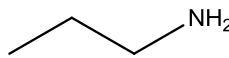
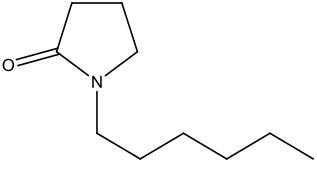
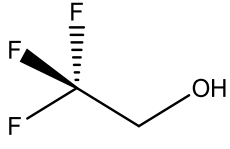
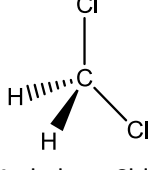
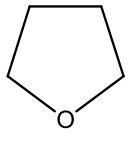
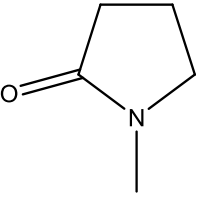
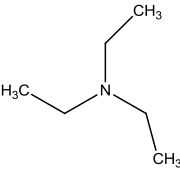
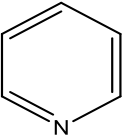
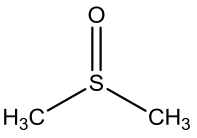
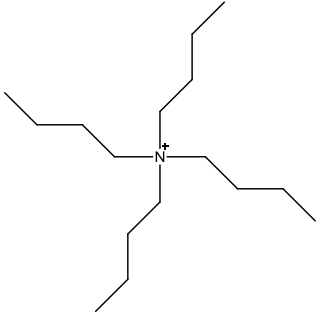
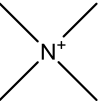
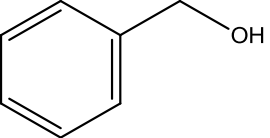
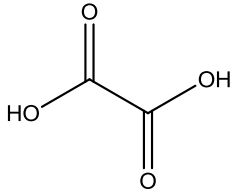
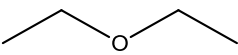
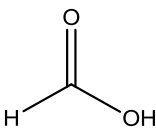
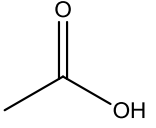


Figure S18. Absorbance data for flowerlike Bi_2WO_6 ($1.6 \times 10^{-5} \text{ M}$) before (black curve) and after (red curve) UV irradiation.

Table S1: Solvent study of Bi₂WO₆ nanosheets dispersed in approximately 5 mL of solvent and irradiated for 2 hrs. The color change afterwards was noted and summarized below.

Solvent	Color change
 Methanol	Black
 propanol	Black
 Butanol	Black
 isopropanol	Black
 Ethylene Glycol	Black
 Water	None
 Acetonitrile	None
 Formamide	None
 ethylamine	Black
 1-hexyl-2-pyrrolidone	None
 2,2,2 trifluoro ethanol	None
 Methylene Chloride	Black
 THF	Black
 None	None

 Triethylamine	Black
 Hexanes	None
 pyridine	None
 DMSO	None
 TBA	Black
 TMA	Black
 Benzyl alcohol	None

 1M Oxalic acid	Black
 diethyl ether	Black
 10% formic acid	Gray
 10% acetic acid	Black
1 M NaOH	None
0.3 M H ₂ SO ₄	None

CsW ₁₁ O ₃₆ nanosheets in TMA	Bluish Black
yellow (restacked) Bi ₂ WO ₆ (Cs) in IPA	Black

Raman spectra were collected with a Renishaw Modu-Laser spectrometer with a diode laser operating at 785 nm. Solid samples were deposited on a quartz slide and run with an acquisition time of 30 s, 0.1% laser power, and a 20x objective lens. Typical resolution was approximately 2 cm^{-1} . The spectrometer was calibrated with an internal Si reference (521 cm^{-1}). Spectra were baseline-corrected in OriginPro 8.5; cosmic ray spikes also were removed using this software.

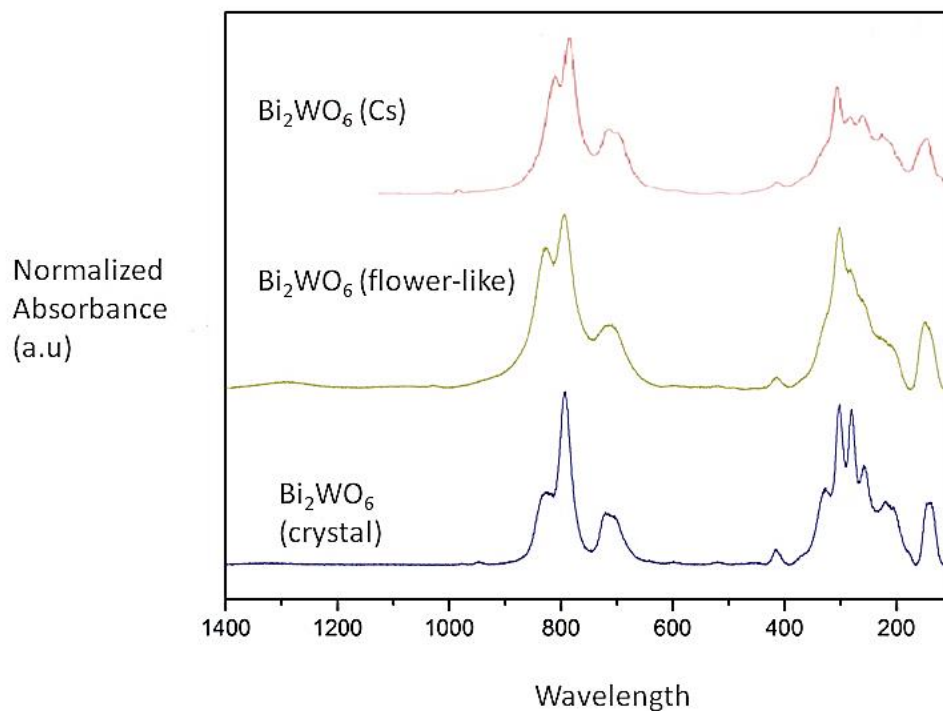


Figure S19. Raman spectra for the three types of Bi₂WO₆ products: Bi₂WO₆ nanosheets derived from Cs₄W₁₁O₃₆²⁻ nanosheets (top red curve), flowerlike Bi₂WO₆ (middle green curve), and single crystal Bi₂WO₆ (bottom blue curve).

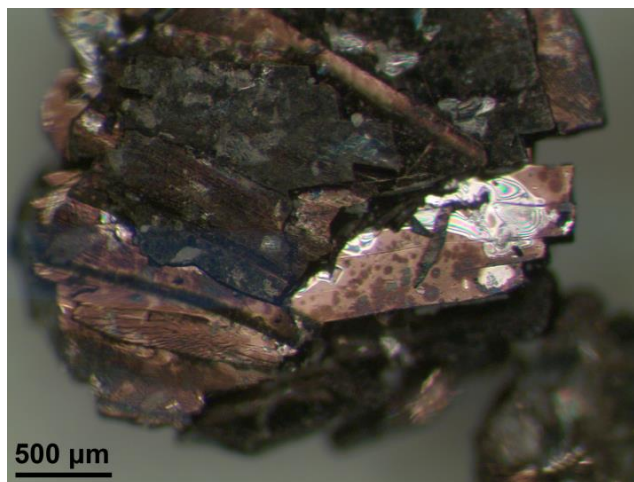


Figure S20. Optical microscopy image of Bi₂WO₆ crystals after lithium intercalation with n-butyllithium.

Preparation of Bi₂WO₆ Single Crystals

This procedure was based on the details reported by Takeda, et al.⁵³ In a typical synthesis, 0.3354 g (1.4 mmol) WO₃ and 0.6676 g (1.4 mmol) Bi₂O₃ were thoroughly mixed together. The powder mixture was calcined in a platinum crucible at 800 °C for 5 hrs. The product was finely ground together with 0.1040 g of Li₂B₄O₇ as the flux. This material was heated to 1,000 °C at a rate of 4 °C per min, then cooled to 940 °C at 10 °C per hr, and then cooled to 840 °C at a rate of 2 °C per hr. Finally the sample was allowed to cool naturally to room temperature. This process resulted in a glossy, yellow-green solid at the bottom of the crucible. The flux was removed with approximately 40 ml of 70% aqueous HNO₃. The yellow crystals remaining were filtered, washed with water, and dried at 105 °C. Isolated yield of Bi₂WO₆ crystals was 0.3287g (32.8%).

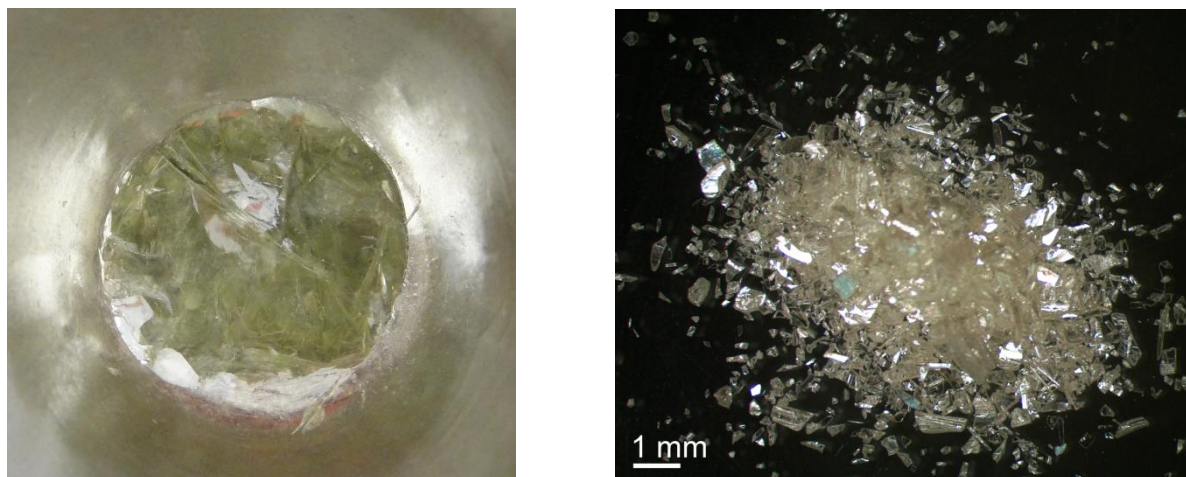


Figure S21. Bi₂WO₆ product in flux (still in platinum crucible at left) and the crystals after leaching and drying (right).

Band Gap Calculation

To calculate the band gap (E_g) the diffuse reflectance data was converted to the Kubelka-Munk function, $F(R_\infty)$, and then used in Tauc's equation. $(h\nu F(R_\infty))^{\frac{1}{n}} = A(h\nu - E_g)$, where $n = 1/2$ for a direct allowed transition, $n = 3/2$ for a direct forbidden transition, $n = 2$ for an indirect allowed transition, $n = 3$ for an indirect forbidden transition, h is Planck's constant, A is a proportional constant, and ν is the frequency of vibration. We plotted $(h\nu F(R_\infty))^{\frac{1}{2}}$ versus $h\nu$ (wavelength converted to eV) and found linear Tauc regions for Bi₂WO₆ (Fig S22). A tangent line was drawn at the inflection point of the curve to provide a horizontal axis intersection point, which is equal to E_g .

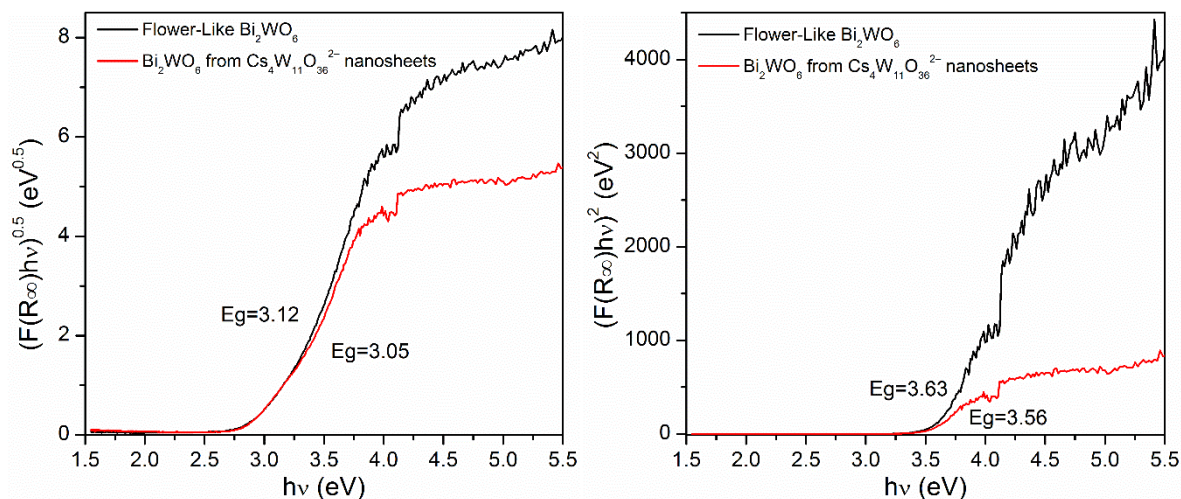


Figure S22. For comparison, Tauc plots of Bi_2WO_6 where $n = 2$ for an indirect allowed transition (left) and $n = 1/2$ for a direct allowed transition (right).

Supplemental Citations

- S1. K. Fukuda, K. Akatsuka, Y. Ebina, R. Ma, K. Takada, I. Nakai and T. Sasaki, *ACS Nano*, **2008**, *2*, 1689-1695.
- S2. (a) C. Zhang and Y. Zhu, *Chem. Mater.*, **2005**, *17*, 3537-3545. (b) L. Zhang, W. Wang, Z. Chen, L. Zhou, H. Xu and W. Zhu, *J. Mater. Chem.*, **2007**, *17*, 2526-2532.
- S3. H. Takeda, J. S. Han, M. Nishida, T. Shiosaki, T. Hoshina and T. Tsurumi, *Solid State Commun.*, **2010**, *150*, 836-839.